

# Planar Curve Interpolation by Piecewise Conics of Arbitrary Type

Robert Schaback

**Abstract:** Five points in general position in  $\mathbb{R}^2$  always lie on a unique conic, and three points plus two tangents also have a unique interpolating conic, the type of which depends on the data. These well-known facts from projective geometry are generalized: an odd number  $2n+1 \geq 5$  of points in  $\mathbb{R}^2$ , if they can be interpolated at all by a smooth curve with nonvanishing curvature, will have a unique  $GC^2$  interpolant consisting of pieces of conics of varying type. This interpolation process reproduces conics of arbitrary type and preserves strict convexity. Under weak additional assumptions its approximation order is  $\mathcal{O}(h^5)$ , where  $h$  is the maximal distance of adjacent data points  $f(t_i)$  sampled from a smooth and regular planar curve  $f$  with nonvanishing curvature. Two algorithms for the construction of the interpolant are suggested, and some examples are presented.

**Keywords:** Geometric rational curve interpolation, shape preservation, convexity, parametric splines, conics, approximation order.

**MSC Classification:** 41A05, 41A15, 41A20, 65D05, 65D07, 65D17, 68U07

## 1 Introduction

Geometric two-point Hermite interpolation of planar curve data by a  $GC^2$  piecewise cubic polynomial interpolant was considered by deBoor, Höllig, and Sabin [2]. The approximation order of their interpolation process is  $\mathcal{O}(h^6)$  for  $h \rightarrow 0$  with respect to the maximal distance  $h$  of adjacent data points, but the interpolant does not always exist. The method of Goodman, Ong, and Unsworth ([4], [5], [6]) avoids this drawback by using rational cubics and is tailored to reproduce arcs of circles. However, its approximation order is not known but does not exceed 4, as can be shown by looking at special cases. For planar Lagrange data, a  $GC^2$  and  $\mathcal{O}(h^4)$  interpolant to convex data, using piecewise quadratic polynomials, was given in [9] with extensions in [10] and [11]. The paper [12] contains  $GC^{k-1}$  methods of order  $\mathcal{O}(h^{2k})$  at the price of using piecewise polynomials of degree  $2k+1$ . Because the high degree causes unwanted wiggles in curvature plots, one should keep the degree of interpolating curves as small as possible. Furthermore, these high-order methods are not generally convexity-preserving. Therefore one should try to achieve the highest possible approximation order using local pieces of low degree without sacrificing shape-preserving properties. An overview of rational geometric interpolation schemes is provided by [13], while non-interpolating rational spline construction methods are given by Boehm [1] and Farin [3]. A cubic rational  $GC^2$  spline interpolant for space curves was designed by Höllig [7].

---

<sup>0</sup>File:  $\tilde{/}$ tex/fertig/rat/trapp.tex, T $\tilde{E}$ Xed on August 31, 1992, Status : Revised for Constructive Approximation

The goal of this paper is to provide a convexity-preserving method for curves in  $\mathbb{R}^2$  that uses piecewise quadratic rational functions, reproduces arbitrary conics and has approximation order  $\mathcal{O}(h^5)$ . Specifically, we assume an odd number  $2n + 1 \geq 3$  of data points  $y_0, y_1, \dots, y_{2n}$  in  $\mathbb{R}^2$  to be given. Then we want to interpolate the data by a geometrically  $C^2$  curve, consisting of pieces

$$r_j(t) := \frac{\sum_{i=0}^2 b_{2j+i} \beta_i(t) w_{ij}}{\sum_{i=0}^2 \beta_i(t) w_{ij}}, \quad t \in [0, 1], \quad 0 \leq j \leq n-1 \quad (1.1)$$

of rational quadratic curves in Bernstein–Bézier representation (see e.g.: [3], [8]), where

$$\beta_i(t) = \binom{2}{i} (1-t)^{2-i} t^i, \quad i = 0, 1, 2$$

are the quadratic Bernstein polynomials and

$$w_{ij} > 0, \quad 0 \leq i \leq 2, \quad 0 \leq j \leq n-1$$

are weights. The control points  $b_i$  for  $i = 0, 1, \dots, 2n$  are to be constructed such that  $r_j$  interpolates the data  $y_{2j}, y_{2j+1}, y_{2j+2}$  on  $[0, 1]$  and a geometrically  $C^2$  continuous curve results, when  $r_0, \dots, r_{n-1}$  are joined together at the data points  $y_2, y_4, \dots, y_{2n-2}$ . This immediately implies

$$b_{2j} = y_{2j}, \quad 0 \leq j \leq n$$

and leaves the construction of the “interior” control points  $b_{2j+1}$  for  $0 \leq j \leq n-1$  open. In the sequel we avoid certain degeneracies by assuming that for each  $j$  the data points  $y_{2j}, y_{2j+1}, y_{2j+2}$  are mutually different. A somewhat stronger assumption will be made in section 3.

Because  $y_{2j+1} \in \mathbb{R}^2$  can be interpolated at an arbitrary parameter value, there is only one additional scalar condition in each piece  $r_j(t)$  to be satisfied. Geometric  $C^2$  continuity imposes two scalar conditions at each junction. There are three degrees of freedom per interval, because  $b_{2j+1} \in \mathbb{R}^2$  and (up to normalization) essentially one weight parameter can be chosen (see [3], [8]). This leaves two degrees of freedom for additional boundary conditions. These are imposed by prescribing tangents at  $y_0$  and  $y_{2n}$ . We later comment on construction methods for these tangents, if they are not given right from the start.

Necessarily, our  $GC^2$  interpolant, if it exists, must have a curvature which vanishes everywhere or nowhere, because each rational piece has this property. Thus our interpolation problem can be solvable only if the data either lie on a straight line or are “strictly convex” in the sense that there is some smooth and regular interpolant to the data with nonvanishing curvature. We shall assume the latter, and then our interpolation process will preserve “strict convexity”, because the curvature of our interpolant will not vanish.

## 2 Local $GC^1$ Hermite interpolation

This section serves as a preparation for later investigations and treats the much simpler problem of local  $GC^1$  two-point Hermite interpolation. Here, an additional tangent direction is prescribed at every even-numbered data point. It is a repeated instance of the special case  $n = 1$  of the problem posed in the previous section, and can be interpreted as a geometric three-point Hermite-Birkhoff interpolation scheme.

To interpolate three data points  $y_0, y_1, y_2$  in  $\mathbb{R}^2$  and two tangent directions  $r_0$  and  $r_2$  at  $y_0$  and  $y_2$ , respectively, by a nondegenerate conic, we again have to assume that the data can be interpolated by a smooth and regular curve with nonvanishing curvature. Thus  $y_1$  should lie inside the triangle defined by  $y_0, y_2$  and the tangents at  $y_0, y_2$  with intersection point  $Q = b_1$ . Note that  $b_1$  will be the interior control point of (1.1) for  $n = 1$  (see Figure 1).

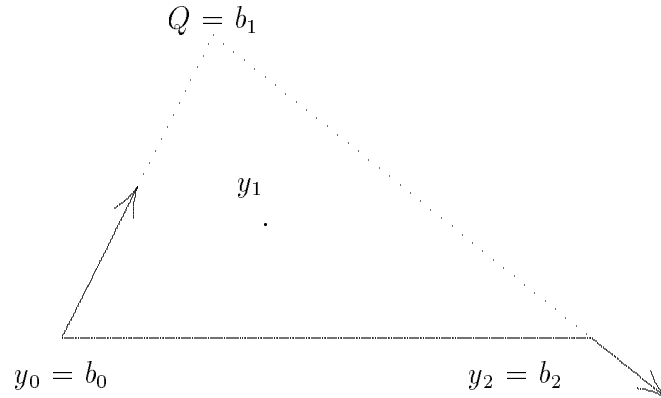


Figure 1: Basic triangle for  $GC^1$  interpolation

It is well known from projective geometry that this problem is uniquely solvable: three points and two tangents uniquely define a conic. The classical construction of an additional point of the conic proceeds as follows:

Take an arbitrary line  $L$  emanating from  $y_0$  and intersecting  $Qy_2$ . Let  $R$  be the intersection of lines  $L$  and  $y_1y_2$ , and construct  $S$  as the intersection of  $QR$  with  $y_0y_1$ . Then the intersection  $P$  of lines  $Sy_2$  and  $L$  is the unique intersection point of  $L$  and the conic within the triangle.

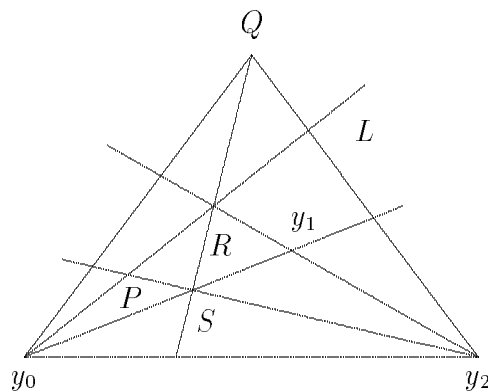


Figure 2: Interpolation for 3 points and two tangents

To derive a direct formula for the solution we observe that there are unique positive real numbers  $\alpha_0, \alpha_2$  with

$$y_1 - b_1 = \alpha_0(b_0 - b_1) + \alpha_2(b_2 - b_1),$$

provided by barycentric coordinates of  $y_1$  with respect to  $b_0, b_2$  and  $b_1$ . From the standard representation by Bernstein polynomials we can write any value  $r(t)$  of a rational quadratic as

$$r(t) - b_1 = \frac{\beta_0(t)(b_0 - b_1) + \beta_2(t)(b_2 - b_1)}{\beta_0(t) + \beta_1(t)w_1 + \beta_2(t)},$$

where we used  $w_0 = w_2 = 1$  without loss of generality (see [8]). If  $r$  interpolates  $y_1$  at the parameter  $t_1$  we get the system

$$\begin{aligned}\alpha_0 &= \frac{\beta_0(t_1)}{\beta_0(t_1) + \beta_1(t_1)w_1 + \beta_2(t_1)}, \\ \alpha_2 &= \frac{\beta_2(t_1)}{\beta_0(t_1) + \beta_1(t_1)w_1 + \beta_2(t_1)}\end{aligned}$$

which is uniquely solved by

$$t_1 = (1 + \sqrt{\alpha_0/\alpha_2})^{-1} \quad (2.1)$$

and

$$w_1 = \frac{1}{2} \frac{1 - \alpha_0 - \alpha_2}{\sqrt{\alpha_0\alpha_2}}. \quad (2.2)$$

This yields a local  $GC^1$  Hermite interpolation method for piecewise conics of arbitrary type which is convexity preserving and reproduces all conics. Its complexity grows linearly with the number of data points.

### 3 Basic Equations for $GC^2$ Interpolation

For a general rational quadratic curve in Bernstein–Bézier representation with control points  $b_0, b_1, b_2$  and weights  $w_0, w_1, w_2$ , we consider arbitrary partitions  $\{i, j, k\}$  of  $\{0, 1, 2\}$  and let  $h_k = \|b_i - b_j\|_2$  be the distance between points  $b_i$  and  $b_j$ , while  $c_k$  is the distance of  $b_k$  to the line  $L_k$  through  $b_i$  and  $b_j$ . Then the curvature at  $b_0$  is ([1], p.71)

$$\kappa_0 = \frac{1}{2} \frac{c_2}{h_2^2} \frac{w_0 w_2}{w_1^2}.$$

Let  $r = r(t)$  be an arbitrary point on the conic. The areas  $A_i$  of the triangles  $r, b_j, b_k$  satisfy

$$\frac{w_0 w_2}{4w_1^2} = \frac{A_0 A_2}{A_1^2}$$

(see [8], p. 10). If  $q_i$  is the distance of  $r$  to the line  $L_i$ , then  $A_i = \frac{1}{2} q_i \cdot h_i$  and

$$\frac{w_0 w_2}{4w_1^2} = \frac{q_0 h_0 q_2 h_2}{q_1^2 h_1^2}.$$

This gives

$$\kappa_0 = 2 \frac{c_2}{h_2^2} \frac{q_0 h_0 q_2 h_2}{q_1^2 h_1^2}, \quad \kappa_2 = 2 \frac{c_0}{h_0^2} \frac{q_0 h_0 q_2 h_2}{q_1^2 h_1^2}$$

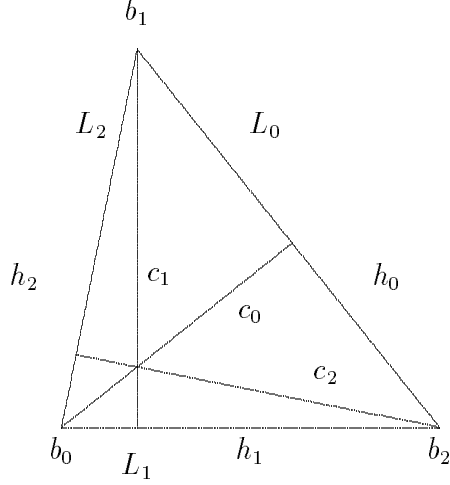


Figure 3: Data for curvature calculation

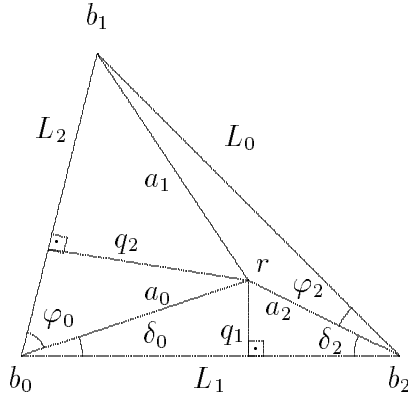


Figure 4: Local angles

for the curvatures  $\kappa_0$  at  $b_0$  and  $\kappa_2$  at  $b_2$ . If  $b_0, r$ , and  $b_2$  are fixed, everything can be expressed by the angles  $\varphi_0, \delta_0$  and  $\varphi_2, \delta_2$  in Figure 4. We introduce  $a_i = \|r - b_i\|$  and find

$$\begin{aligned} \frac{q_2}{a_0} &= \sin \varphi_0 & \frac{q_0}{a_2} &= \sin \varphi_2 \\ \frac{q_1}{a_0} &= \sin \delta_0 & \frac{q_1}{a_2} &= \sin \delta_2 \\ \frac{c_1}{h_2} &= \sin(\varphi_0 + \delta_0) = \frac{c_2}{h_1}, & \frac{c_1}{h_0} &= \sin(\varphi_2 + \delta_2) = \frac{c_0}{h_1}, \end{aligned}$$

the last two equations following from Figure 3. This implies

$$\begin{aligned} \kappa_0 &= \frac{2 \sin(\varphi_0 + \delta_0)}{h_2} \cdot \frac{h_0 \sin \varphi_2 \sin \varphi_0}{h_1 \sin \delta_0 \sin \delta_2} \\ &= \frac{2 \sin(\varphi_0 + \delta_0) \sin \varphi_2 \sin \varphi_0}{\sin \delta_0 \sin \delta_2} \cdot \frac{\sin(\varphi_0 + \delta_0)}{h_1 \sin(\varphi_2 + \delta_2)} \\ &= \frac{2 \sin \varphi_0 \cdot \sin \varphi_2}{h_1 \sin \delta_0 \cdot \sin \delta_2} \frac{\sin^2(\varphi_0 + \delta_0)}{\sin(\varphi_2 + \delta_2)}, \end{aligned} \tag{3.1}$$

and similarly

$$\kappa_2 = \frac{2}{h_1} \frac{\sin \varphi_0 \cdot \sin \varphi_2}{\sin \delta_0 \sin \delta_2} \frac{\sin^2(\varphi_2 + \delta_2)}{\sin(\varphi_0 + \delta_0)}. \quad (3.2)$$

Furthermore,

$$\kappa_2 = \kappa_0 \left( \frac{\sin(\varphi_2 + \delta_2)}{\sin(\varphi_0 + \delta_0)} \right)^3. \quad (3.3)$$

Before we proceed, we remark that it is not generally possible to prescribe three points and two curvature values to define a conic, in spite of the analogous fact that three points with two tangent directions uniquely determine a conic. In fact, if  $\kappa_0$  and  $\kappa_2$  were prescribed together with  $b_0, r$ , and  $b_1$ , there are two equations (3.2) and (3.3) for the two unknowns  $\varphi_0$  and  $\varphi_2$ . However, these equations are not necessarily solvable, as can be seen in the special symmetric case  $\kappa = \kappa_0 = \kappa_2$ ,  $\delta = \delta_0 = \delta_2$ , where (3.3) implies  $\varphi_0 = \varphi_2$  and (3.2) requires

$$\kappa = \frac{2}{h_1} \frac{\sin^2 \varphi}{\sin^2 \delta} \sin(\varphi + \delta),$$

which is an unsolvable equation in case

$$\kappa h_1 \sin^2 \delta > 2,$$

for example. Note that this negative result corresponds to the similar one in [2].

We now proceed to use (3.1) and (3.2) to express curvature continuity around a point  $y_{2i}$  for the  $GC^2$  interpolation problem posed in the introduction. In order to let the geometric construction of Fig. 5 be well-defined, we assume the restrictions

$$\begin{aligned} 0 &< \delta_i^+, & 0 &< \delta_i^-, \quad 1 \leq i \leq n, \\ 0 &< \delta_i^+ + \delta_i^- < \gamma_i < \pi, \quad 1 \leq i \leq n-1 \\ 0 &< \varphi_0^+ < \varphi_0^+ + \delta_0^+ < \pi, \\ 0 &< \varphi_n^- < \varphi_n^- + \delta_n^- < \pi, \end{aligned} \quad (3.4)$$

on the given data, where  $\gamma_i$  is the angle between the chords  $y_{2i-2}y_{2i}$  and  $y_{2i}y_{2i+2}$ . Furthermore, the varying angles  $\varphi_i^-$  and  $\varphi_i^+$  should satisfy

$$\varphi_i^-, \varphi_i^+ > 0, \quad \varphi_i^+ + \varphi_i^- + \delta_i^- + \delta_i^+ = \gamma_i, \quad 1 \leq i \leq n-1.$$

Note that these restrictions are always satisfied if the data form a sufficiently dense sample from a smooth regular curve with nonvanishing curvature.

Curvature continuity  $\kappa_i^- = \kappa_i^+$  at  $y_{2i}$  in Fig. 5 implies

$$\begin{aligned} \kappa_i^- &= \frac{2}{h_{i-1}} \frac{\sin \varphi_{i-1}^+ \sin \varphi_i^-}{\sin \delta_{i-1}^+ \sin \delta_i^-} \frac{\sin^2(\varphi_i^- + \delta_i^-)}{\sin(\varphi_{i-1}^+ + \delta_{i-1}^+)} \\ = \kappa_i^+ &= \frac{2}{h_i} \frac{\sin \varphi_i^+ \sin \varphi_{i+1}^-}{\sin \delta_i^+ \sin \delta_{i+1}^-} \frac{\sin^2(\varphi_i^+ + \delta_i^+)}{\sin(\varphi_{i+1}^- + \delta_{i+1}^-)}, \quad 1 \leq i \leq n-1 \end{aligned}$$

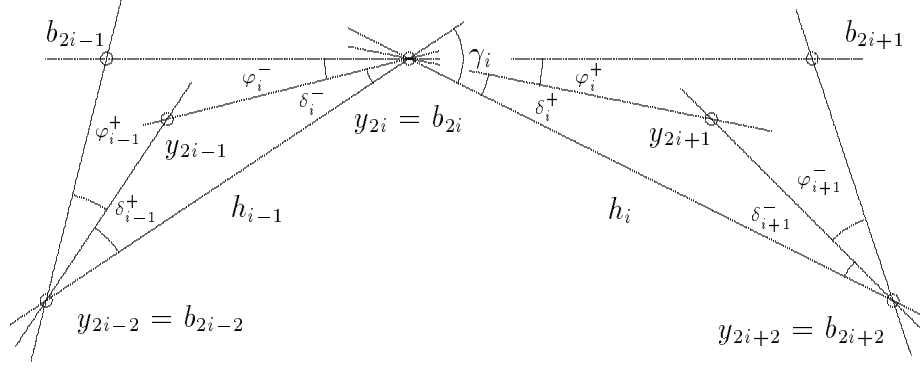


Figure 5: Local angles around  $y_{2i}$

and, with  $\varphi_i^+ + \delta_i^+ + \varphi_i^- + \delta_i^- = \gamma_i$ ,  $\varphi_i := \varphi_i^+$  we get

$$\begin{aligned} & \frac{2}{h_{i-1}} \frac{\sin \varphi_{i-1} \sin(\gamma_i - \delta_i^- - \delta_i^+ - \varphi_i)}{\sin \delta_{i-1}^+ \sin \delta_i^-} \cdot \frac{\sin^2(\gamma_i - \varphi_i - \delta_i^+)}{\sin(\varphi_{i-1} + \delta_{i-1}^+)} \\ &= \frac{2}{h_i} \frac{\sin \varphi_i \sin(\gamma_{i+1} - \delta_{i+1}^- - \delta_{i+1}^+ - \varphi_{i+1})}{\sin \delta_i^+ \sin \delta_{i+1}^-} \cdot \frac{\sin^2(\varphi_i + \delta_i^+)}{\sin(\gamma_{i+1} - \varphi_{i+1} - \delta_{i+1}^+)}. \end{aligned} \quad (3.5)$$

This is a nonlinear system of equations in unknowns  $\varphi_1, \dots, \varphi_{n-1}$ . Two boundary tangents must be prescribed by fixing  $\varphi_0^+$  and  $\varphi_n^-$ , and to make the system (3.5) formally valid for  $i = 1$  and  $i = n - 1$ , we define

$$\varphi_0^- = \delta_0^- = 0, \quad \varphi_n^+ = \delta_n^+ = 0, \quad \gamma_0 = \varphi_0^+ + \delta_0^+, \quad \gamma_n = \varphi_n^- + \delta_n^-.$$

The Jacobian of the system is tridiagonal.

## 4 Existence of a $GC^2$ interpolant

Our main result of this section will be

**Theorem 4.1** *Under the conditions (3.4) there is a solution to the interpolation problem.*

For uniqueness we require in addition that

$$\gamma_i < \frac{\pi}{2}, \quad 1 \leq i \leq n \quad (4.1)$$

to get

**Theorem 4.2** *The conditions (3.4) and (4.1) imply uniqueness of the interpolant.*

The rest of this section is devoted to the proof of Theorems 4.1 and 4.2. As a preparation, we state the monotonicity of

$$\sin \varphi \cdot \sin^2(\varphi + \alpha)$$

in both variables  $\varphi, \alpha$  within

$$0 < \varphi < \frac{\pi}{2}, \quad 0 < \alpha < \frac{\pi}{2}, \quad 0 < \varphi + \alpha < \frac{\pi}{2}.$$

Furthermore,

$$f_\alpha(\varphi) = \frac{\sin \varphi}{\sin(\varphi + \alpha)} \quad \text{with} \quad f'_\alpha(\varphi) = \frac{\sin \alpha}{\sin^2(\varphi + \alpha)}$$

is monotonic in  $\varphi$  for all  $\alpha$  with  $0 < \alpha < \pi$ , and covers  $(0, \infty)$  when  $\varphi$  varies over  $(0, \pi - \alpha)$ .

The simultaneous proof of Theorems 4.1 and 4.2 proceeds by inductively checking the range of the nonlinear mapping  $(\varphi_{i-1}, \varphi_i) \mapsto \varphi_{i+1}$  given by (3.5) when interpreted as an implicit definition of  $\varphi_{i+1}$  for given values of  $\varphi_i$  and  $\varphi_{i-1}$ . Uniqueness will be a consequence of strict monotonicity.

We start with a fixed value of  $\varphi_0^+$  (given as a boundary condition) and satisfying the assumptions (3.4). The equation  $\kappa_1^- = \kappa_1^+$  is

$$\begin{aligned} \kappa_1^- &= \frac{2}{h_0} \frac{\sin \varphi_0^+}{\sin \delta_0^+} \frac{\sin \varphi_1^-}{\sin \delta_1^-} \frac{\sin^2(\varphi_1^- + \delta_1^-)}{\sin(\varphi_0^+ + \delta_0^+)} \\ &= \frac{2}{h_1} \frac{\sin \varphi_1^+}{\sin \delta_1^+} \frac{\sin \varphi_2^-}{\sin \delta_2^-} \frac{\sin^2(\varphi_1^+ + \delta_1^+)}{\sin(\varphi_2^- + \delta_2^-)} = \kappa_1^+, \end{aligned}$$

and  $\kappa_1^-$  varies in an interval of the form  $(0, \hat{\kappa}_1)$  when  $\varphi_1^-$  varies in  $(0, \gamma_1 - \delta_1^- - \delta_1^+)$ . Because of  $\varphi_1^- + \varphi_1^+ = \gamma_1 - \delta_1^- - \delta_1^+$ , the variable  $\varphi_1^+$  varies also in  $(0, \gamma_1 - \delta_1^+ - \delta_1^-)$ , but in the opposite direction to  $\varphi_1^-$ . As a function of  $\varphi_1^-$  and  $\varphi_1^+ = \gamma_1 - \delta_1^+ - \delta_1^- - \varphi_1^-$ , the left-hand-side of the expression

$$\frac{h_1}{h_0} \cdot \frac{\sin \delta_1^+ \sin \delta_2^-}{\sin \delta_0^+ \sin \delta_1^-} \cdot \frac{\sin \varphi_1^+}{\sin(\varphi_1^+ + \delta_1^+)} \cdot \frac{\sin \varphi_1^-}{\sin \varphi_1^+} \cdot \frac{\sin^2(\varphi_1^- + \delta_1^-)}{\sin^2(\varphi_1^+ + \delta_1^+)} = \frac{\sin \varphi_2^-}{\sin(\varphi_2^- + \delta_2^-)} = f_{\delta_2^-}(\varphi_2^-) \quad (4.2)$$

covers all of  $(0, \infty)$ . Thus, (4.2) is solvable for  $\varphi_2^-$ , and  $\varphi_2^-$  covers  $(0, \pi - \delta_2^-)$  when  $\varphi_1^-$  varies in  $(0, \gamma_1 - \delta_1^+ - \delta_1^-)$ . Note that all variations are strictly monotonic under the additional assumption (4.1).

Now we have to discard all values of  $\varphi_2^-$  in the interval  $[\gamma_2 - \delta_2^- - \delta_2^+, \pi - \delta_2^-)$ , but surely there is an interval of the form  $(0, \varepsilon_1)$  with  $0 < \varepsilon_1 < \gamma_1 - \delta_1^+ - \delta_1^-$  such that  $\varphi_2^-$  varies over all of  $(0, \gamma_2 - \delta_2^+ - \delta_2^-)$  when  $\varphi_1^-$  varies over  $(0, \varepsilon_1)$ . Furthermore,  $\varphi_2^- = \mathcal{O}(\varphi_1^-)$  for  $\varphi_1^- \rightarrow 0$ .

We now proceed inductively for  $i \geq 2$  and assume the existence of an interval  $(0, \varepsilon_{i-1})$  such that when  $\varphi_1^-$  varies in  $(0, \varepsilon_{i-1})$ , the variable  $\varphi_i^-$  varies over all of  $(0, \gamma_i - \delta_i^+ - \delta_i^-)$  and all of the  $\varphi_j^-$  vary in subintervals  $(0, \rho_j)$  with  $\rho_j < \gamma_j - \delta_j^+ - \delta_j^-$ , while all equations  $\kappa_j^- = \kappa_j^+$  for  $1 \leq j \leq i-1$  are satisfied. Furthermore, all  $\varphi_j^-$  for  $2 \leq j \leq i$  are supposed to satisfy  $\varphi_j^- = \mathcal{O}(\varphi_1^-)$  for  $\varphi_1^- \rightarrow 0$ .

The equation  $\kappa_i^+ = \kappa_i^-$  is equivalent to

$$\frac{h_i}{h_{i-1}} \cdot \frac{\sin \delta_i^+ \sin \delta_{i+1}^-}{\sin \delta_{i-1}^+ \sin \delta_i^-} \cdot \frac{\sin \varphi_{i-1}^+}{\sin(\varphi_{i-1}^+ + \delta_{i-1}^+)} \cdot \frac{\sin \varphi_i^-}{\sin \varphi_i^+} \cdot \frac{\sin^2(\varphi_i^- + \delta_i^-)}{\sin^2(\varphi_i^+ + \delta_i^+)} = \frac{\sin \varphi_{i+1}^-}{\sin(\varphi_{i+1}^- + \delta_{i+1}^-)} = f_{\delta_{i+1}^-}(\varphi_{i+1}^-), \quad (4.3)$$

and again the left-hand side will cover all of  $(0, \infty)$  when  $\varphi_i^-$  and  $\varphi_i^+ = \gamma_i - \delta_i^+ - \delta_i^- - \varphi_i^-$  vary over  $(0, \gamma_i - \delta_i^+ - \delta_i^-)$  in opposite direction. This allows  $\varphi_{i+1}^-$  to solve (4.3) while varying in  $(0, \pi - \delta_{i+1}^-)$ , and we have to discard the values of  $\varphi_{i+1}^-$  in  $[\gamma_{i+1} - \delta_{i+1}^+ - \delta_{i+1}^-, \pi - \delta_{i+1}^-)$  by



restricting  $\varphi_i^-$  to some interval  $(0, \rho_i)$  with  $0 < \rho_i < \gamma_i - \delta_i^+ - \delta_i^-$ . If we denote the left-hand side of (4.3) by  $g_i(\varphi_i^-)$ , we can take the value

$$\rho_i := \inf\{\rho \mid 0 < \rho < \gamma_i - \delta_i^+ - \delta_i^-, \quad g_i(\rho) = f_{\delta_{i+1}^-}(\gamma_{i+1} - \delta_{i+1}^+ - \delta_{i+1}^-)\}$$

for this purpose, making use of  $g_i(\varphi_i^-) = \mathcal{O}(\varphi_i^-) = \mathcal{O}(\varphi_1^-)$  for  $\varphi_1^- \rightarrow 0$  and  $f_{\delta_{i+1}^-}(\varphi_{i+1}^-) = \mathcal{O}(\varphi_{i+1}^-)$  for  $\varphi_{i+1}^- \rightarrow 0$ . This, in turn, will require some positive  $\varepsilon_i < \varepsilon_{i-1}$  to restrict  $\varphi_1^-$  to an interval  $(0, \varepsilon_i)$ . Furthermore,  $\varphi_{i+1}^- = \mathcal{O}(\varphi_i^-) = \mathcal{O}(\varphi_1^-)$  for  $\varphi_1^- \rightarrow 0$ , and the induction step is complete.

For  $i + 1 = n$  we find that  $\varphi_n^-$  covers all of  $(0, \pi - \delta_n^-)$  when  $\varphi_1^-$  varies over  $(0, \varepsilon_{n-1})$ . Therefore, any boundary tangent at the other end of the data set can be prescribed, and there always is a solution.

The assumptions (4.1) guarantee strict monotonicity in each step of the proof. This proves uniqueness of the solution.  $\square$

## 5 Boundary Conditions

As is well known from projective geometry, five given points in general position in a plane will lie on a unique conic. This immediately yields simple and efficient strategies for determining end tangents, which, in addition, will preserve reproduction of conics.

For completeness we include the simple recipe here. If points  $y_0, y_1, \dots, y_4 \in \mathbb{R}^2$  are given, we suggest to program a function

$$F : \mathbb{R}^2 \times \mathbb{R}^2 \times \mathbb{R}^2 \times \mathbb{R}^2 \rightarrow \mathbb{R}^2$$

such that  $F(a, b, c, d)$  is the intersection point of the lines through  $a, b$ , and  $c, d$ , respectively. Then the function calls

$$a := F(y_0, y_2, y_1, y_4)$$

$$b := F(y_0, y_1, y_2, y_4)$$

$$c := F(y_0, y_2, y_3, y_4)$$

$$d := F(y_0, y_3, y_2, y_4)$$

$$s := F(a, b, c, d)$$

generate a point  $s$  such that  $y_0, s, y_4$  are the control points of the interpolating conic in Bernstein-Bézier representation. This immediately yields the tangents to the conic at  $y_0$  and  $y_4$ . If the weight  $w_1$  or the parameters of  $y_1, y_2, y_3$  are required, use the  $GC^1$  two-point Hermite construction of section 2. Note that the above construction, when naively programmed in  $\mathbb{R}^2$  as described here, will fail whenever the given points are not in general position. Going over to projective geometry will remedy the situation somewhat and will produce tangents at  $y_0$  and  $y_4$ , even if some of the lines are parallel. However, for sufficiently dense data samples from smooth planar curves with nonvanishing curvature there will be no problems.

This basic construction can be easily adapted to generate convexity-preserving boundary tangents at  $y_0$  and  $y_{2n}$  from  $y_0, \dots, y_4$  and  $y_{2n-4}, \dots, y_{2n}$ . Then we have a  $GC^2$  Lagrange interpolation method which preserves convexity and all conics. If we use the local five-point construction for estimation of tangents in the  $GC^1$  case, we end up with the same properties.

A given boundary tangent at  $y_0$  can be viewed as a twofold data point; thus it seems reasonable to look for a method that replaces tangent data at  $y_0$  by an additional data point  $y_{-1}$ . This strategy is similar to the “not-a-knot” boundary condition for nonparametric spline interpolation. For all conics through  $y_{-1}, y_0, y_1, y_2$  the control point  $P$  of the rational Bézier representation in terms of  $y_{-1}, P$ , and  $y_2$  must lie on the upper part of the line  $AB$  of Figure 6 (compare with Figure 2).

This can be used to relate the angles  $\varphi_2^-$  and  $\varphi_{-1}^+$ , which in turn makes it possible to write the curvature  $\kappa_2^-$  at  $y_2$  as a complicated function of  $\varphi_2^-$  alone. But then the system (3.5) does not require a boundary condition for  $\varphi_0^+$ . An existence proof for the solution can be given by the topological techniques of [9], but we omit the details here, because it is much simpler to apply the previously proposed five-point method.

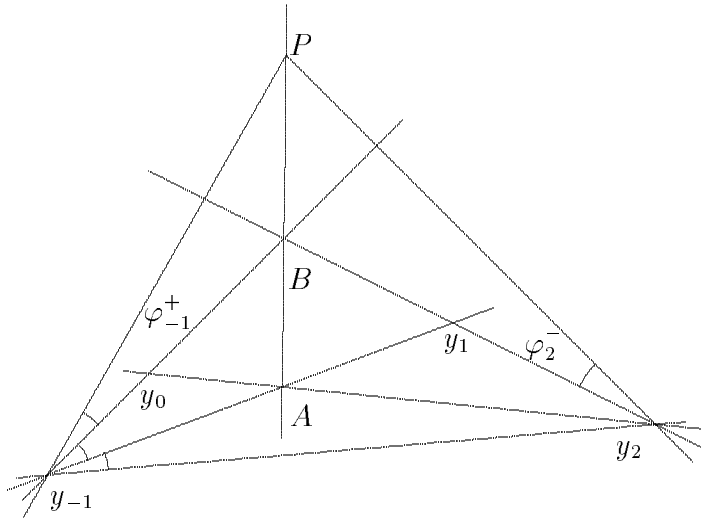


Figure 6: not-a-knot condition

We conclude this section by pointing out that the five-point method can also be used to generate an additional data point that fits in with conic precision, making it possible to assume that the number of data points always is odd, provided that it is at least 5.

## 6 Convergence

Numerical experiments suggest  $\mathcal{O}(h^5)$  accuracy of the interpolation process as described above, if the data  $y_i = f(t_i)$ ,  $0 \leq i \leq 2n$  are sampled from a smooth and regular curve  $f : [a, b] \subset \mathbb{R} \rightarrow \mathbb{R}^2$  with nonvanishing curvature, where

$$h := \min_{1 \leq i \leq 2n} (t_i - t_{i-1}), \quad a \leq t_0 < t_1 < \dots < t_{2n} \leq b$$

tends to zero. The technique of the  $\mathcal{O}(h^4)$  convergence proof of [9] for piecewise quadratic polynomial  $GC^2$  interpolation can be carried over to this situation. It requires a thorough analysis of a scaled version of the underlying nonlinear system and applies a Newton-Kantorovitch type theorem with the following main ingredients:

- The system must behave like  $\mathcal{O}(h^3)$  for exact data from  $f$  to get  $\mathcal{O}(h^5)$  accuracy of the interpolant.
- The original variables should be scaled by a factor with behavior  $\mathcal{O}(h^{-1})$ .
- The scaled system must have a uniform bound for the inverse of its Jacobian, and
- its second derivatives must be uniformly bounded for  $h \rightarrow 0$ .

The final result will be

**Theorem 6.1** *For sufficiently dense samples of data  $y_i = f(t_i)$  from a regular and sufficiently smooth curve  $f$  with nonvanishing curvature, and for uniformly bounded ratios*

$$0 < \gamma \leq \frac{\|f(t_{2i}) - f(t_{2i\pm 1})\|}{\|f(t_{2i}) - f(t_{2i\pm 2})\|} \leq 1 - \gamma, \quad 1 \leq i \leq n - 1 \quad (6.1)$$

with a fixed value of  $\gamma \in (0, 1)$ , the interpolation process of the preceding sections has  $\mathcal{O}(h^5)$  accuracy.

**Proof:** As in [9], there are some complicated expansions to be calculated. So let  $f : [a, b] \rightarrow \mathbb{R}^2$  be a smooth planar curve with positive curvature, parametrized by arclength. We can follow [2] and [9] to assume a local two-dimensional representation of  $f$  around a single point by

$$f(0) = \begin{pmatrix} 0 \\ 0 \end{pmatrix}, \quad f'(t) = \begin{pmatrix} \cos \theta(t) \\ \sin \theta(t) \end{pmatrix}$$

$$\theta(t) = \sum_{i=1}^{k-1} \theta_i t^i + \mathcal{O}(t^k) \quad (6.2)$$

without loss of generality. Here  $\theta(t)$  is the angle between tangents of  $f$  at  $f(0)$  and  $f(t)$ , while the curvature at  $f(t)$  is

$$\kappa(t) = \theta'(t) = \sum_{i=1}^{k-1} i \theta_i t^{i-1} + \mathcal{O}(t^{k-1}).$$

The angle  $\alpha(t)$  between the chord  $f(t) - f(0)$  and the tangent to  $f$  at  $f(0)$  can be expanded as

$$\alpha(t) = \frac{1}{2}\theta_1 t + \frac{1}{3}\theta_2 t^2 + \frac{1}{4}\theta_3 t^3 + \frac{72\theta_4 - \theta_1^2\theta_2}{360}t^4 + \frac{120\theta_5 - 4\theta_1\theta_2^2 - 3\theta_1^2\theta_3}{720}t^5 + \mathcal{O}(t^6) \quad (6.3)$$

for  $t \rightarrow 0$  by a straightforward REDUCE program based on the expansion (6.2) of  $\theta(t)$ . Here and in the sequel the expansions will be truncated for simplicity of typesetting and reading; it is no major problem to extend them by appropriate calculations with any software system for symbolic computation.

Further analysis of the system (3.5) along the lines of [9] requires the angle

$$\begin{aligned} \rho(t, u) = & \frac{1}{2}\theta_1(t+u) + \frac{1}{3}\theta_2(t^2+ut+u^2) + \frac{1}{4}\theta_3(t^3+t^2u+tu^2+u^3) + \\ & \frac{72\theta_4 - \theta_1^2\theta_2}{360}(t^4+u^4) + \frac{18\theta_4 + \theta_1^2\theta_2}{90}(t^3u+tu^3) + \frac{12\theta_4 - \theta_1^2\theta_2}{60}t^2u^2 + \\ & \frac{120\theta_5 - 4\theta_1\theta_2^2 - 3\theta_1^2\theta_3}{720}(t^5+u^5) + \frac{40\theta_5 + 4\theta_1\theta_2^2 + 3\theta_1^2\theta_3}{240}(t^4u+tu^4) + \\ & \frac{60\theta_5 - 4\theta_1\theta_2^2 - 3\theta_1^2\theta_3}{360}(t^3u^2+t^2u^3) + \mathcal{O}(t^6) + \mathcal{O}(u^6) \end{aligned}$$

between the tangent at  $f(0)$  and the chord through  $f(t)$  and  $f(u)$ . Note that

$$\rho(t, u) = \begin{cases} \alpha(t) & u = 0 \\ \alpha(u) & t = 0 \\ \theta(t) & u = t \end{cases}, \quad (6.4)$$

and we shall assume  $0 < u < t$  throughout. The second part of the system (3.5) can now be rewritten in a simpler form: the correspondences are

$$\begin{aligned} y_{2i} &= f(0), & y_{2i+1} &= f(u), & y_{2i+2} &= f(t), \\ \varphi_i^+ &= \alpha(u), & \delta_i^+ &= \alpha(t) - \alpha(u), & \varphi_i^+ + \delta_i^+ &= \alpha(t), \\ \varphi_{i+1}^- &= \theta(t) - \rho(t, u), & \delta_{i+1}^- &= \rho(t, u) - \alpha(t), & \varphi_{i+1}^- + \delta_{i+1}^- &= \theta(t) - \alpha(t), \\ h_i &= c(t), & & & \|y_{2i+1} - y_{2i}\|_2 &= c(u), \end{aligned}$$

where

$$\begin{aligned} c(t) &= t - \frac{\theta_1^2}{24}t^3 - \frac{\theta_1\theta_2}{12}t^4 + \frac{3\theta_1^4 - 432\theta_1\theta_3 - 256\theta_2^2}{5760}t^5 \\ &\quad + \frac{\theta_1^3\theta_2 - 32\theta_1\theta_4 - 40\theta_2\theta_3}{480}t^6 + \mathcal{O}(t^7) \end{aligned}$$

is the chordlength  $\|f(t) - f(0)\|_2$  as a function of arclength  $t$ . After inserting the expansions of the angles in Taylor series of sines, and after expansion of denominators by application of Neumann's series there is a representation

$$\begin{aligned} \kappa^+(t, u) &= \theta_1 + t^2(\kappa_{2,1}u + \mathcal{O}(u^2)) + u\mathcal{O}(t^3) + \mathcal{O}(t^4) \\ \kappa_{2,1} &= (18\theta_1^4\theta_2 + 54\theta_1^2\theta_4 - 135\theta_1\theta_2\theta_3 + 80\theta_2^3)/(135\theta_2^2) \end{aligned} \quad (6.5)$$

for the right-hand part of the curvature in (3.5). Therefore (3.5) vanishes like  $\mathcal{O}(h^3)$  for data from a smooth and regular curve. Note that the corresponding system in [9] had a system that vanished like  $\mathcal{O}(h^2)$ , giving overall  $\mathcal{O}(h^4)$  accuracy of the interpolation. No dramatic effect of  $u$  being near to 0 or to  $t$  arises at this point, because the ratios

$$\begin{aligned} \frac{\varphi_i^+}{\delta_{i+1}^-} &= \frac{\alpha(u)}{\rho(t, u) - \alpha(t)} = \frac{u\theta_1/2 + u^2\theta_2/3 + \mathcal{O}(u^3)}{u\theta_1/2 + u(t+u)\theta_2/3 + u\mathcal{O}(t^2)} \\ \frac{\varphi_{i+1}^-}{\delta_i^+} &= \frac{\theta(t) - \rho(t, u)}{\alpha(t) - \alpha(u)} = \\ &\quad \frac{(t-u)\theta_1/2 + (t-u)(2t+u)\theta_2/3 + (t-u)\mathcal{O}(t^2)}{(t-u)\theta_1/2 + (t-u)(t+u)\theta_2/3 + (t-u)\mathcal{O}(t^2)} \end{aligned}$$

tend to 1 even if the denominators vanish (see (6.4) for the other cases). The remaining terms of  $\kappa^+(t, u)$  are functions of  $t$  alone.

We now proceed to analyze partial derivatives of a properly scaled version of the system (3.5). Expansion (6.5) shows that (3.5) will vanish cubically with  $t \rightarrow 0$ , yielding degenerate Jacobians in the limit. To care for this, we scale the variables in a suitable way, using  $\psi_i := \varphi_i/u_i$  instead of  $\varphi_i = \varphi_i^+$ , where

$$u_i^- := \|y_{2i-1} - y_{2i}\|, \quad u_i^+ := \|y_{2i} - y_{2i+1}\|, \quad u_i := \min(u_i^+, u_i^-).$$

Note that these numbers are fixed within a single interpolation problem; they can be treated as constants when taking derivatives. Then we have

$$\frac{\partial \kappa^+}{\partial \psi_i} = \frac{u_i}{u} u \frac{\partial \kappa^+}{\partial \varphi_i}$$

and

$$\frac{\partial \kappa^+}{\partial \psi_{i+1}} = \frac{u_{i+1}}{t-u} (t-u) \frac{\partial \kappa^+}{\partial \varphi_{i+1}} = -\frac{u_{i+1}}{t-u} (t-u) \frac{\partial \kappa^+}{\partial \varphi_{i+1}^-}.$$

The latter derivatives can be expanded into

$$\begin{aligned} u \frac{\partial \kappa^+}{\partial \varphi_i} &= 2 + 4 \frac{u}{t} + \mathcal{O}(u) + \mathcal{O}(t^4) \\ (t-u) \frac{\partial \kappa^+}{\partial \varphi_{i+1}^-} &= 2 \frac{u}{t} + \mathcal{O}(u). \end{aligned}$$

Due to (6.1) and

$$\begin{aligned} \frac{u_i}{u} &\leq 1 + \mathcal{O}(t), & \frac{u_{i+1}}{t-u} &\leq 1 + \mathcal{O}(t), \\ 2 \frac{u}{t} &\leq 2 - 2\gamma + \varepsilon, & 2 + 4\gamma - \varepsilon &\leq 2 + 4 \frac{u}{t} \end{aligned}$$

for any given  $\varepsilon > 0$  and sufficiently small  $t > u > 0$ , the Jacobian  $J$  of (3.5) will be strictly diagonally dominant and satisfy

$$\|J\|_\infty \leq 16, \quad \|J^{-1}\|_\infty \leq \frac{1}{12\gamma}$$

for  $t \rightarrow 0$ . The second derivatives can be shown to be bounded for  $t \rightarrow 0$ , using a similar expansion together with the proposed scaling. The rest of the proof, applying a Kantorovich type convergence theorem for Newton's method, precisely follows the lines of [9].  $\square$

## 7 Numerical treatment

As in [9], the asymptotic considerations of the convergence analysis suggest a modified Newton–Raphson method with stepsize control for solving the nonlinear system (3.5). The same paper provides convexity-preserving starting values of order  $\mathcal{O}(h^3)$ , and the technique of [12] yields derivative estimates of arbitrarily high order. The latter are not necessarily convexity-preserving in all cases, but due to their high order they will preserve convexity for sufficiently small  $h$ . So there will be no major problems when solving (3.5) with a safeguarded Newton–Raphson technique.

The  $- + -$  sign distribution and the strict diagonal dominance of the tridiagonal Jacobian makes a simple Gauss-Seidel iteration applicable around the solution. This worked rather well in practice, especially when combined with starting values from tangents which were estimated using the five-point method of section 5. The difference between this  $GC^1$  interpolant and the final  $GC^2$  interpolant often is graphically invisible, but of course the curvature plots show the difference. In anticipation of possible numerical problems with the various sines occurring in (3.5), a simple univariate zero-finding procedure with linear convergence was employed to solve (3.5) for  $\varphi_i$ . Repeating this process cyclically over  $i$  proved to be efficient enough.

## 8 Examples

To illustrate the  $\mathcal{O}(h^5)$  convergence, we sampled  $2n + 1 = 2^{k+1} + 1$  points (plus two boundary tangents) of a 90 degree arc of a logarithmic spiral  $f$  with exponent  $-0.25$  at equidistant (non-arclength) parameter values. The rational interpolants to these data were sampled at 513 points at equidistant parameter values of their piecewise rational Bernstein–Bézier representation, giving  $2^{8-k} - 1$  interior points in each of the  $n - 1 = 2^k - 1$  pieces. To each of these points of the interpolant, the nearest point of  $f$  was calculated by a simple minimization routine, yielding the discrete  $L_\infty$  errors given in Table 1. In spite of the rather crude technique of error measurement, the results clearly show an error reduction of about  $1/32$  when doubling the number of data points.

$n$	$L_\infty$ error
2	$2.212_{10} - 5$
4	$8.739_{10} - 7$
8	$2.689_{10} - 8$
16	$8.494_{10} - 10$
32	$2.660_{10} - 11$

Table 1: Errors of interpolation to logarithmic spiral

Due to the high approximation order, plots of interpolants practically always reproduce the interpolated curve within plot precision, if the data are sampled from a smooth curve. In such cases, curvature plots give much more information; a number of examples of this type can be found in [13], comparing this method with other rational interpolants.

Here we provide results for some coarse data sets which were manually entered without smoothing. Boundary tangents were estimated by the five-point formula of section 5. Of course, data sets with four or less points cannot be handled by our method, and data sets with five points will automatically yield the unique conic that fits through these five points. Thus, at least seven points are needed for nontrivial examples.

Figure 7 contains a plot of the  $GC^2$  interpolant to seven data points in convex position, while the corresponding curvature plot is given in Figure 8. Note that the interpolant consists of only three pieces, as shown in the curvature plot.

The last example, given in Figures 9 and 10, has 19 points in the shape of an @ letter. Here, the curve takes a left turn, making the right part of the curvature plot correspond to the lower part of the curve.

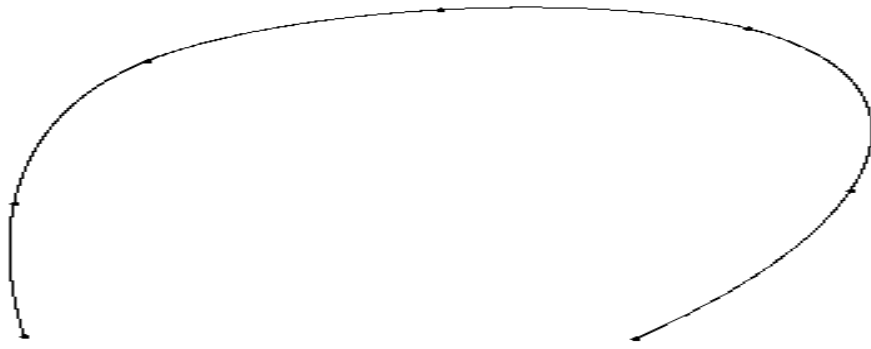


Figure 7: Seven data points with  $GC^2$  interpolant

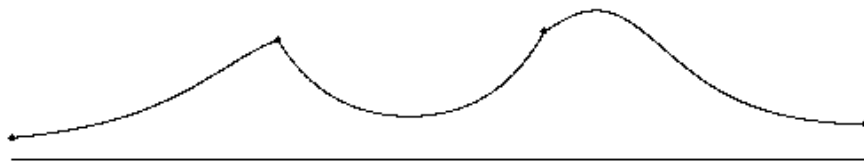


Figure 8: Curvature of  $GC^2$  interpolant



Figure 9: Nineteen data points with  $GC^2$  interpolant

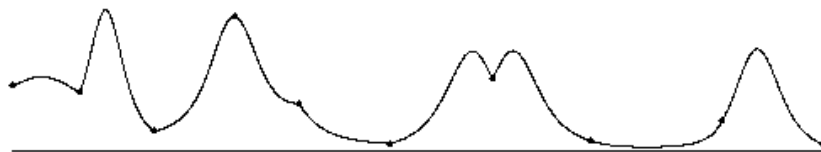


Figure 10: Curvature of  $GC^2$  interpolant

## References

- [1] BOEHM, W., Rational geometric splines, *Comput. Aided Geom. Design* **4** (1987) 67-78
- [2] DEBOOR, C., HÖLLIG, K., AND SABIN, M., High Accuracy Geometric Hermite Interpolation, *Computer Aided Geometric Design* **4** (1987) 269-278
- [3] FARIN, G.E. Rational curves and surfaces, *Mathematical Methods in Computer Aided Geometric Design*, Tom Lyche and L. L. Schumaker (eds.), Academic Press, New York, 1989, 215-238
- [4] GOODMAN, T. N. T., Shape preserving interpolation by parametric rational cubic splines, *Numerical Mathematics Singapore 1988*, R. P. Agarwal, Y. M. Chow, and S. J. Wilson (eds.), International Series of Numerical Mathematics, Vol. 86, Birkhäuser, Basel, 1988, 149-158
- [5] GOODMAN, T. N. T., B. H. ONG, K. UNSWORTH, Constrained interpolation using rational cubic splines, Univ. of Dundee, Computer Sciences Report CS90/01, 1990
- [6] GOODMAN, T. N. T., K. UNSWORTH, An algorithm for generating shape preserving parametric interpolating curves using rational cubic splines, Univ. of Dundee, Computer Sciences Report CS89/01, 1989
- [7] HÖLLIG, K., Algorithms for Rational Spline Curves, ARO-Report 88-1, 1988, 287-300
- [8] LEE, E. T., The rational Bézier representation of conics in Geometric Modeling, *Geometric Modeling: Algorithms and New Trends*, G. Farin (ed.), SIAM, Philadelphia, 1987, 3-19
- [9] SCHABACK, R., Interpolation in  $\mathbb{R}^2$  by piecewise quadratic visually  $C^2$  Bezier polynomials, *Computer Aided Geometric Design* **6** (1989) 219-233
- [10] SCHABACK, R., On Global  $GC^2$  Convexity Preserving Interpolation of Planar Curves by Piecewise Bezier Polynomials, in T. Lyche and L.L. Schumaker (eds.): "Mathematical Methods in Computer Aided Geometric Design", Academic Press 1989, 539-547
- [11] SCHABACK, R., Convergence of Planar Curve Interpolation Schemes, in C.K. Chui, L.L. Schumaker and J.D. Ward (eds): "Approximation Theory VI", 1989, 581-584
- [12] SCHABACK, R., Geometric Differentiation and High-Accuracy Curve Interpolation, to appear in S.N. Singh (ed.): *Approximation Theory, Splines, and Applications*, Proceedings of a NATO-ASI conference, Maratea 1991
- [13] SCHABACK, R., Rational Curve Interpolation to appear in T. Lyche and L.L. Schumaker (eds.): "Mathematical Methods in Computer Aided Geometric Design II", Academic Press 1992

Author's address:



Prof. Dr. R. Schaback  
Institut für Numerische und Angewandte Mathematik  
Lotzestraße 16–18

D–3400 Göttingen